Impact of size-dependent non-local elastic strain on the electronic band structure of embedded quantum dots

P Sharma and **X Zhang**
1 Department of Mechanical Engineering, University of Houston, Houston, Texas, USA
2 Department of Physics, University of Houston, Houston, Texas, USA

The manuscript was received on 06 May 2006 and was accepted after revision for publication on 09 April 2006.

DOI: 10.1243/17403499JNN57

Abstract: The effect of mechanical strain on the quantum confinement properties of quantum dots is appreciable and both qualitative and quantitative description of the electronic band structure of quantum dots requires proper incorporation of its effect. Although atomistic calculations such as tight binding or pseudopotential approaches are viable options, the typical and 'standard' practice is to employ the coarse-grained multiband envelope function method to compute the band structure of both strained and unstrained quantum dots. The typical recipe involves calculation of strain based on classical continuum elasticity and a subsequent link to the aforementioned eight-band envelope function model. The mechanical strain predicted by classical elasticity is not only size-independent but also departs qualitatively from the actual (atomistic) field owing to neglect of non-local effects that are prevalent at the nanoscale. In the present work, the authors employ the strain as calculated from a size-dependent non-local theory of elasticity (presented in work previously published by the current authors) and assess the qualitative and quantitative effects on the electronic band structure of an InAs-GaAs quantum dot system. Quantitatively, deviations of band gaps in the range of 100 meV are found when compared to classical elasticity-based estimates, while no significant qualitative differences were found. The non-local elastic effects, however, are appreciable only for very small quantum dots and certain materials (such as the InAs–GaAs system discussed in the present work).

Keywords:

1 INTRODUCTION AND BACKGROUND

Quantum dots are tiny three-dimensionally confined (typically) semiconductor material structures where quantum effects become obvious, e.g. energy spectra become discrete. They are characterized by sharp density of states reminiscent of 'atoms' and carriers are confined in all three dimensions. Quantum dots are of immense technological importance and (while several technological barriers remain) are often considered as the basis for several revolutionary nanoelectronic devices and applications, e.g. next generation lighting [**1, 2**], lasers [**3, 4**], quantum computing, information storage and quantum cryptography [**5–7**], biological labels [**8**], sensors [**9**], and many others.

As is routinely done in quantum structure research, size can be used to tailor or engineer the electronic spectra and hence a host of other optoelectronic properties in quantum dots or wires/wells. For example (while somewhat crude), a single-band effective mass particle-in-a-box approximation immediately suggests that band gaps vary as $E_g(R) = E_g(\infty) + k/R^2$ where E_g is the band gap, while 'R' is some characteristic dimension of the quantum dot, e.g. radius for a spherical one. Numerically, the proportionality constant, k, (which involves effective masses, Planck's constants, etc.) is such that hardly any size effect or quantum confinement is seen until the quantum dot dimensions approach a few nanometres (or more formally the exciton Bohr radius). Apart from many other interesting aspects of electronic behaviour of

**Corresponding author: Department of Mechanical Engineering, Engineering Building One, University of Houston, Houston, Texas, 77204-4006, USA. email: psharma@uh.edu*

three-dimensionally confined quantum dots (cf. reference [**10**]), the ability to tailor the band structure with minute changes in size (at the nanoscale) is perhaps the one that is most often emphasized.

Insofar as the strain is concerned, quantum dots are frequently embedded in another material with different elastic constants and lattice parameters. In such a case, owing to the lattice mismatch, the ensuing elastic strain within the quantum dots is well known to impact their optoelectronic properties (e.g. references [**10–13**]). For example, the mismatch strain between InAs and GaAs is 7 per cent. Thus, in addition to quantum dot size, mechanical strain also has an influence on the band structure. Strain can shift the valence and conduction bands, change band gap, cause trapping of carriers and excitons, and in some piezoelectric materials even cause (e.g. group III–V materials) electrical fields that further impact the optoelectronic properties of quantum dots. Although the major effect is attributable to dilatational strain, axial components can break the cubic symmetry (of most semiconductors) and lead to splitting of the light and heavy hole bands. Again, this aspect of strain-mediated control of electronic properties is well known and indeed employed to alter the band structure of both bulk systems and nanostructures.

A wide range of band structure calculation approaches is available, ranging from all-electron methods to approximate *ab initio* approaches [self-consistent density functional theory (DFT), the empirical pseudopotential method (EPM), tight binding (TB), or the envelope function method (EFM). Within each category, sub-methods of varying sophistication can be readily identified. The reader is referred to references [**11–14**], which provide decent overviews. For example, EFM, which in its so-called standard 8×8 Hamiltonian (Kane model [**15**]) is the most often used, involves taking into account the influence of the three energy bands on the valence side and one on the conduction side leading to a set of 8×8 Schrödinger-type equations that must be solved numerically for the energy eigenvalues. In this model, spin–orbital coupling, light–heavy hole band mixing, as well as non-parabolicity of electron dispersion is included. Indeed this model has been frequently applied to quantum dots [e.g. references **16–21**]. Significant progress has been made in the development of this method even for quantum dot heterostructures (see the progress by various researchers made in references [**22–33**]). In principle, this approach is exact if *all energy bands* (not just four) are retained. The simple particle in a box effective mass approach corresponds to a single band approximation. Mechanical strain can be accounted for in the Kane model as a perturbation (e.g. references [**11–14, 21, 34**]) and such modifications typically result in a further complication of the 8×8 standard Hamiltonian albeit that is readily tractable numerically. In this formalism, non-homogeneous strains may also be dealt with rigorously via the work of Zhang [**35**].

Typically strain itself is usually calculated via recourse to continuum elasticity (numerically or analytically depending on geometrical and anisotropic assumptions) and sometimes through empirical force field molecular dynamics (e.g. references [**36–67**]). The envelope function approach is attractive, simple, and physically intuitive and thus not surprisingly a 'standard' approach utilized in most works on both bulk semiconductors as well as nanostructures. However, this 'standard approach' suffers from several shortcomings and its applicability to nanostructures appears questionable. Indeed, several authors have discussed this (e.g. see review by DiCarlo [**68**]) and alternative 'more microscopic' approaches such as TB, EPM, or DFT are often preferable when dealing with small quantum dots in the size range of a few nanometres. In various works Zunger and co-workers [**69–71**] have highlighted and clarified the various shortcomings of the envelope function approach when compared with EPM calculations. Wang and Zunger [**70,71**] have made an important advance by modifying the 'standard' envelope function approach to be accurate for small quantum dots. While the EPM is fairly accurate provided the pseudopotential that replaces the effect of core electrons/nucleus has been well tweaked empirically, it is computationally expensive for large systems (underscoring somewhat the importance of the work by Wang and Zunger [**70, 71**] on the modification of the k.p model for quantum dots). Self-consistent DFT computations, which while parameter-free often tend to underestimate the energies as DFT, are best suited for only ground state energy calculation. Even within DFT, accuracy may suffer if the typically used local density approximation is utilized as opposed to incorporation of non-local effects. Nevertheless, relative effects are often faithfully captured by DFT and its advantage of being parameter-free is notable for new materials and effects. Applications are, however, generally limited to quantum dots below 2.5 nm and indeed embedded systems often prove to be beyond computational reach.

In the present work, the authors acknowledge that classical elasticity predictions of mechanical strain in embedded quantum dots are in error both qualitatively and for some materials quantitatively as well (for the size range of 2–10 nm). Physically, owing to the non-local effects prevalent at the nanoscale, strain is *size-dependent* in contrast to classical elasticity predictions. The calculation of the size-dependent strain in embedded quantum dots has been

explored in greater depth in one of the present authors' recent works through the use of the phenomenological strain gradient theory of elasticity [**72**]. Crude calculations indeed showed that the consequence on band structure of some materials systems (such as InAs–GaAs) may be non-negligible. In the present work, a detailed study is provided of the issue of strain-band structure coupling in InAs–GaAs quantum dots whereby the strain is calculated through the non-local theory of elasticity. Given the intent of this paper, it is somewhat immaterial whether an isotropic assumption is made for the strain calculations. In any event, a few works do claim that the inclusion of anisotropy only has negligible effect [**37–38**]. In the present authors' opinion, this certainly may not be the case for all materials. Anisotropic non-local elasticity calculations have already been carried out in a previous work [**72**] and thus, to keep matters simple, isotropic elasticity is assumed. Note that interfacial energy effects may also cause an additional size dependency [**11, 73**] that is not discussed in the present work.

The current paper is organized as follows. In section 2, the strain field calculation based on size-dependent strain gradient elasticity (as presented in reference [**72**]) is briefly recapitulated. In section 3, the eight-band model for electronic band structure calculations of strained quantum dots is discussed and the authors' computational scheme is briefly explained. Numerical results are presented and discussed in section 4, while conclusions are given in section 5.

2 SIZE-DEPENDENT STRAIN OWING TO NON-LOCAL EFFECTS

This section is based on the authors' previous work [**72**] and the reader is referred to that work for more details on the relevant derivations. The authors note here as motivation that at small length scales (approaching a few nanometres comparable to the discrete structure of matter) the implicit long-wavelength assumption of classical elasticity breaks down. This breakdown is caused partially by fluctuations in the inter-atomic interactions at the length scale of a few lattice spacings that are smoothed out at coarser scales (where classical elasticity is reasonably applicable). As one would expect, several phenomena at the level of a few lattice spacings are inadequately captured by classical elasticity and researchers often see enriched continuum theories such as non-local elasticity as a replacement for atomistic simulations (or alternatively a bridge between atomistic and conventional continuum mechanics). For example, the ubiquitous singularities ahead of crack tips and dislocation cores (as predicted by classical mechanics) are indeed a breakdown of traditional elasticity at short wavelengths [**74**]. The obvious alternative method to compute strain is the use of atomistic simulations. An alternative (coarse-grained) field theoretical method is highly desirable (in the same vein as previous works [**38, 39, 42–46, 75**]), albeit one that also accounts for the scaling or size effects in strain likely to be prevalent at these small length scales (over and beyond surface/interfacial energy effects already addressed in the references [**73, 75, 76**]).

Non-local elasticity is formulated by using modified energy density [**77**]. Extra terms related to strain gradients are introduced

$$W(\mathbf{x}) = \mu(\partial_i u_j)^2 + \frac{\lambda}{2}(\partial_l u_l)^2 + \frac{2\mu+\lambda}{2} l'^2 \partial_i\partial_l u_l \partial_i\partial_j u_j + \frac{\mu l^2}{2}\left(\partial_l^2 u_i \partial_l^2 u_i - \partial_i\partial_l u_l \partial_i\partial_j u_j\right) \quad (1)$$

Here, the first two quadratic terms form the classical energy density; μ and λ are shear modulus and Lame's modulus of elastic medium. It is presumed that the energy density would not only depend on strain but also on strain gradient. Additional material parameters (in addition to the Lame parameters) now appear, namely l' and l (the so-called characteristic length scales). Here, u_i is the displacement and is related to strain ε_{ij} via

$$\varepsilon_{ij} = \frac{1}{2}(u_{i,j} + u_{j,i})$$

∂_i is equivalent to $\partial/\partial x_i$ and the two notations will be used interchangeably to indicate differentiation with respect to the spatial variables. Assume that a lattice mismatch strain exists between the embedded quantum dots and the host matrix. The mismatch strain, ε^{m} in terms of the lattice parameters is given as

$$\varepsilon_{ij}^{\mathrm{m}} = \frac{2(a_{\mathrm{qd}} - a_{\mathrm{host}})}{(a_{\mathrm{qd}} + a_{\mathrm{host}})}\delta_{ij} = \varepsilon^{\mathrm{m}}\delta_{ij} \quad (2)$$

where a_{qd} and a_{host} are lattice parameters for quantum dot and matrix material; δ_{ij} is the Kronecker delta.

For the simple spherical shape, closed-form results can be derived for the size-dependent strain [**72**]

$$\varepsilon_{ii}(r) = \begin{cases} \frac{\Xi}{3} + \Xi e^{-\frac{R_0}{l'}}(R_0 + l')\frac{Fin(x_i)}{r^5} & \in \Omega \\ \frac{i\Xi R_0^3}{3r^5} Fou_1(x_i) + \Xi L e^{-r/l'}\frac{Fou_2(x_i)}{r^5} & \notin \Omega \end{cases}$$
$$\varepsilon_{jk}(r) = 0, \qquad k \neq j \quad (3)$$

where

$$\Xi = \frac{3\lambda + 2\mu}{\lambda + 2\mu}$$

Additional unknown terms in the above function are defined as

$$
\begin{aligned}
Fin(x_i) = {} & l' r\left(2x_i^2 - x_j^2 - x_k^2\right)\cosh\frac{r}{l'} \\
& - \sinh\frac{r}{l'}\left[l'^2\left(2x_i^2 - x_j^2 - x_k^2\right) + x_i^2 r^2\right] \quad i \neq k \neq j \\
Fou_1(x_i) = {} & -2x_i^2 + x_j^2 + x_k^2 \qquad i \neq k \neq j \\
Fou_2(x_i) = {} & \left[l'^2\left(x_j^2 + x_k^2 - 2x_i^2\right)\right. \\
& \left. -l' r\left(2x_i^2 - x_j^2 - x_k^2\right) - x_i^2 r^2\right] \qquad i \neq k \neq j \\
L = {} & l' \sinh\frac{R_0}{l'} - R_0 \cosh\frac{R_0}{l'}
\end{aligned} \tag{4}
$$

The classical elasticity solution may be recovered by simply letting the length scale tend to zero

$$
\begin{aligned}
\varepsilon_{ii}(r) &= \begin{cases} \frac{\Xi}{3} & \in \Omega \\ \frac{\Xi R_0^3}{3r^5} Fou_1(x_i) & \notin \Omega \end{cases} \\
\varepsilon_{jk}(r) &= 0, \qquad k \neq j
\end{aligned} \tag{5}
$$

The classical and non-local strain fields are compared in Figs 1 and 2.

In both Figs 1 and 2, the strain is normalized as $Tr(\varepsilon_{ij})(3K + 4\mu)/9K\varepsilon^{\mathrm{m}}$. Figure 1 emphasizes the size dependency of non-local elasticity. The results are plotted for various positions inside the quantum dot. It can be seen from sub-plot (a) that the size dependency of strain is prominent for a quantum dot with radius less than $6l'$. Because the internal length scale is usually very small (see discussion in section 3), the non-local effect should be appreciable for small quantum dots. Large deviation can exist for even 'large' quantum dots near the interface of the quantum dot and matrix. Figure 2 shows another important feature of non-local elasticity that which is the total strain is continuous across the boundary. Unlike the classical result, which is a constant dilation inside the quantum dot and zero outside, the non-local strain dilation is non-uniform both inside and outside the quantum dot and continuous. This is more physical. It also needs to be emphasized that non-local elasticity removes singularity of the strain field at the vertices of polyhedral-shaped quantum dots [**72**].

After duly subtracting mismatch strain inside the quantum dot [**50**], the strain fields obtained in equations (4) and (5) will be used in the following section for band structure calculations.

3 BAND STRUCTURE CALCULATION FOR InAs–GaAs QUANTUM DOT SYSTEM

A typical procedure, used for zinc blende semiconductors in several references, is to employ the eight-band envelope function framework. Most work essentially uses the Bir–Pikus [**78**] Hamiltonian or some modification of it. The reader is referred to Bahder [**79**] and Pollak [**34**] for good reviews of this

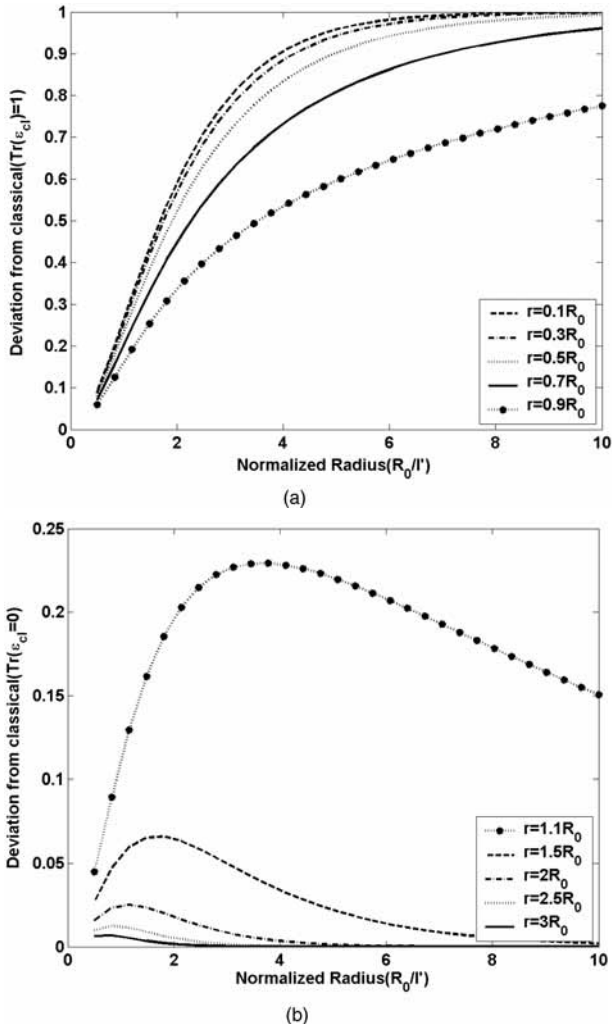

Fig. 1 Dilatational strain in non-local elasticity: size dependency of strain. (a) Inside the quantum dot: classical strain dilation is normalized as 1. The results are plotted for various positions inside the quantum dot. (b) Outside the quantum dot: classical strain dilation is zero

subject, in addition to the book by Singh [**12**]. Several other works can be consulted as well, which utilize this multiband k.p approach (e.g. references [**20, 60, 80**]).

The starting point for the eight-band model that incorporates the effect of strain is the following single-particle Schrodinger's equation [**71**]

$$
-\frac{\hbar^2}{2m}\nabla^2\psi(\mathbf{r}) + V(\mathbf{r})\psi(\mathbf{r}) + W_{\mathrm{strain}}\psi(\mathbf{r}) = E\psi(\mathbf{r}) \tag{6}
$$

Here V is extra potential induced by the external field and W is a coupling potential caused by the strain field. By incorporating the spin–orbital coupling effect, equation (6) is re-written as [**71**]

$$
\begin{aligned}
& -\frac{\hbar^2}{2m}\nabla^2\psi(\mathbf{r}) + V(\mathbf{r})\psi(\mathbf{r}) + +W_{\mathrm{strain}}\psi(\mathbf{r}) \\
& + \frac{\hbar}{4c^2m^2}(\nabla V \times \mathbf{p}) \quad \sigma = E\psi(\mathbf{r})
\end{aligned} \tag{7}
$$

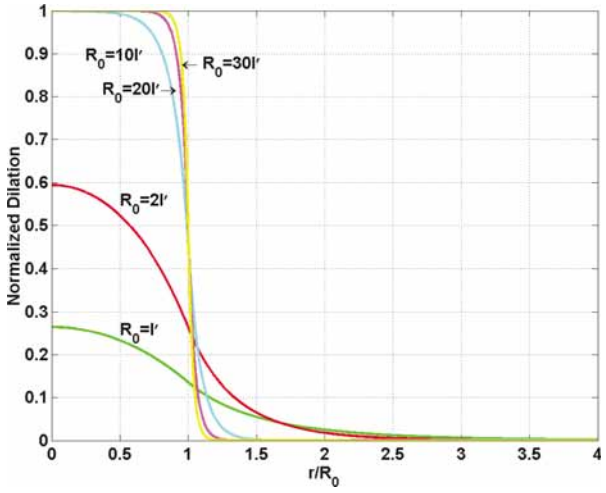

Fig. 2 Dilatational strain distribution in non-local elasticity plotted for various quantum dot sizes

Where V is the potential energy term of the Hamiltonian, $\mathbf{p}$ is the momentum operator, and σ is the Pauli spin tensor. The wave function can be expanded in terms of the so-called envelope functions [**71**]

$$\psi(\mathbf{r}) = \sum_{n=1}^{N_b} \left[\sum_k b_n(\mathbf{k}) e^{i\mathbf{k}\quad \mathbf{r}} \right] \phi_{n,\mathbf{k}=0}(\mathbf{r}) \tag{8}$$

Here N_b is the number of energy bands. N_b is 1 for a single-band model (conduction band and valence band), or 8 for a standard 8×8 envelope function method. $\phi_{n,\ \mathbf{k}=0}(\mathbf{r})$ is the atomic function near the Γ point.

$$F_n(r) = \sum_k b_n(\mathbf{k}) e^{i\mathbf{k}\quad \mathbf{r}},$$

is the slowly varying envelope function. With the linear expansion given in equation (8), equations (6) and (7) are expanded into the N_b band model. The derivation from equation (7) in multiband formulae is well known [**80**] hence using this directly, the following can be written:

$$\sum_{m=1}^{N_b} \psi(\mathbf{r}) = \sum_{n=1}^{N_b} \left[\left(E_{n,0} + \frac{\hbar^2 k^2}{2m_0} - E_{n,k} \right) \delta_{m,n} + \frac{\hbar}{m_0} \mathbf{KP}_{n,m} + W_{nm} \right] b_m(k) = 0 \tag{9}$$

where W_{nm} represent the linear expansion coefficients in multiband coordinates for the strain coupling part. The above equation could be transformed into a more familiar form by adding $\sum_k e^{i\mathbf{k}\,\mathbf{r}}$ to both sides. Finally, the following can be written

$$\sum_m (H_{nm}(\mathbf{r}) + W_{nm}(\mathbf{r})) F_m(\mathbf{r}) = EF_n \tag{10}$$

$H_{nm}(\mathbf{r})$ can be written as [**20, 81**]

$$\mathbf{H}_{nm} = \begin{bmatrix} A & 0 & V^* & 0 & \sqrt{3}V & -\sqrt{2}U & -U & \sqrt{2}V^* \\ 0 & A & -\sqrt{2}U & -\sqrt{3}V^* & 0 & -V & \sqrt{2}V & U \\ V & -\sqrt{2}U & -P+Q & -S^* & R & 0 & \sqrt{\frac{3}{2}}S & -\sqrt{2}Q \\ 0 & -\sqrt{3}V & -S & -P-Q & 0 & R & -\sqrt{2}R & \frac{1}{\sqrt{2}}S \\ \sqrt{3}V^* & 0 & R^* & 0 & -P-Q & S^* & \frac{1}{\sqrt{2}}S^* & \sqrt{2}R^* \\ -\sqrt{2}U & -V^* & 0 & R^* & S & -P+Q & \sqrt{2}Q & \sqrt{\frac{3}{2}}S^* \\ -U & \sqrt{2}V^* & \sqrt{\frac{3}{2}}S^* & -\sqrt{2}R^* & \frac{1}{\sqrt{2}}S & \sqrt{2}Q & -P-\Delta & 0 \\ \sqrt{2}V & U & -\sqrt{2}Q & \frac{1}{\sqrt{2}}S^* & \sqrt{2}R & \sqrt{\frac{3}{2}}S & 0 & -P-\Delta \end{bmatrix} \tag{11}$$

The terms in the above equation are differential operators and are defined as

$$\begin{aligned} A &= E_c - \frac{\hbar^2 \alpha}{2m} \nabla^2 \\ P &= -E_v - \gamma_1 \frac{\hbar^2}{2m} \nabla^2 \\ Q &= -\gamma_2 \frac{\hbar^2}{2m} \left(\partial_x^2 + \partial_y^2 - 2\partial_z^2 \right) \\ R &= \sqrt{3} \frac{\hbar^2}{2m} \left[\gamma_2 \left(\partial_x^2 - \partial_y^2 \right) - 2i\gamma_3 \partial_x \partial_y \right] \\ S &= -\sqrt{3}\gamma_3 \frac{\hbar^2}{2m} \partial_z (\partial_x - i\partial_y) \\ U &= \frac{-i}{\sqrt{3}} P_0 \partial_z \\ V &= \frac{-i}{\sqrt{6}} P_0 (\partial_x - i\partial_y) \end{aligned} \tag{12}$$

The strain coupling Hamiltonian has the following form

$$\mathbf{W}_{nm} = \begin{bmatrix} a_c e & 0 & -v^* & 0 & -\sqrt{3}v & \sqrt{2}u & u & -\sqrt{2}v^* \\ 0 & a_c e & \sqrt{2}u & \sqrt{3}v^* & 0 & v & -\sqrt{2}v & -u \\ -v & \sqrt{2}u & -p+q & -s^* & r & 0 & \sqrt{\frac{3}{2}}s & -\sqrt{2}q \\ 0 & \sqrt{3}v & -s & -p-q & 0 & r & -\sqrt{2}r & \frac{1}{\sqrt{2}}s \\ -\sqrt{3}v^* & 0 & r^* & 0 & -p-q & s^* & \frac{1}{\sqrt{2}}s^* & \sqrt{2}r^* \\ \sqrt{2}u & v^* & 0 & r^* & s & -p+q & \sqrt{2}q & \sqrt{\frac{3}{2}}s^* \\ u & -\sqrt{2}v^* & \sqrt{\frac{3}{2}}s^* & -\sqrt{2}r^* & \frac{1}{\sqrt{2}}s & \sqrt{2}q & -a_v e & 0 \\ -\sqrt{2}v & -u & -\sqrt{2}q & \frac{1}{\sqrt{2}}s^* & \sqrt{2}r & \sqrt{\frac{3}{2}}s & 0 & -a_v e \end{bmatrix} \tag{13}$$

Similarly, the terms in above matrix are defined as

$$\begin{aligned} p &= a_v (e_{xx} + e_{yy} + e_{zz}) \\ q &= b \left[e_{zz} - \frac{1}{2} (e_{xx} + e_{yy}) \right] \\ r &= \frac{\sqrt{3}}{2} b (e_{xx} - e_{yy}) - ide_{xy} \\ s &= -d (e_{xz} - ie_{yz}) \\ u &= \frac{-i}{\sqrt{3}} P_0 \sum_j e_{zj} \partial_j \\ v &= \frac{-i}{\sqrt{6}} P_0 \sum_j (e_{xj} - ie_{yj}) \partial_j \end{aligned} \tag{14}$$

Where m is the mass of a bare electron and $\hbar$ is the modified Planck's constant. The required relevant parameters for the InAs–GaAs system are summarized in Table 1.

Another important parameter is the valence band offset, which in the current study is chosen to be 0.27 eV [**10, 21, 82**]. In order to incorporate the non-local size-dependent strain, the length scale parameter l' needs to be fixed. Clearly, the numerical values of the characteristic length scale determine the strength of the non-local or dispersive behaviour of the crystal. Eringen [**74**] provides an elementary discussion of this length scale. Of course this parameter is different for different materials. Generally the rough magnitude of this length scale is around the lattice parameter. Realistic values can only be obtained using detailed atomistic simulations. However, a crude one-dimensional Born–Karman type chain model (presented by Eringen [**74**]; pages 100–101) indicates this parameter to be exactly equal to the lattice parameter ('a'). Further, Eringen also indicates (page 107) that matching non-local theories to experimental phonon dispersion curves yields $l = 0.39a$ (unfortunately he does not specify which material, other than indicating that it is of face-centred cubic structure). Altan and Aifantis [**60**] suggest a similar number. A better way to resolve this matter is through detailed lattice level models. DiVincenzo [**83**] precisely appears to have done so. In fact he addresses dispersivity (non-locality) in the semiconductor material GaAs. To understand this issue further, a discussion of a key concept is in order. As used in the present authors' earlier works [**72**], for GaAs the length scale is taken to be roughly ~ 0.832 nm. In any event, since there is some uncertainty surrounding this number, a sample calculation is also provided based on a much smaller value $\sim a/2$ (see Fig. 4 in section 4).

Table 1 Band structure calculation parameters [**83**]

Parameter	GaAs*	InAs*
$\boldsymbol{K}$ (GPa)	75.3	78.1
γ_1	7.10	19.7
γ_2	2.02	8.4
γ_3	2.93	9.3
E_g (eV)	1.518	0.413
Δ (eV)	0.34	0.38
E_p (eV)	28.0	22.0
a_c (eV)	−8.01	−5.08
a_v (eV)	−0.22	−1.00
b (eV)	−1.824	−1.8
d (eV)	−5.062	−3.6
C_{1111} (GPa)	121.1	83.3
C_{1122} (GPa)	54.8	45.3
C_{1212} (GPa)	60.4	39.6

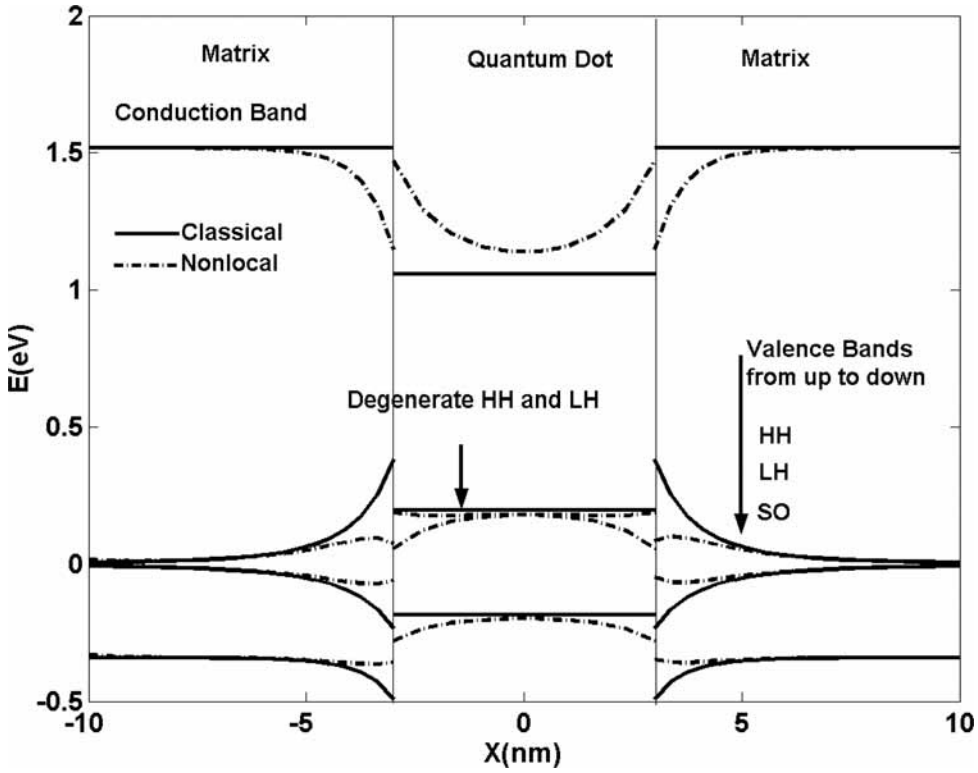

Fig. 3 Band edge profile for quantum dot heterogeneous system (InAs–GaAs) with conduction band and valence bands [heavy hole (HH); light hole (LH); spin–orbital (SO)]

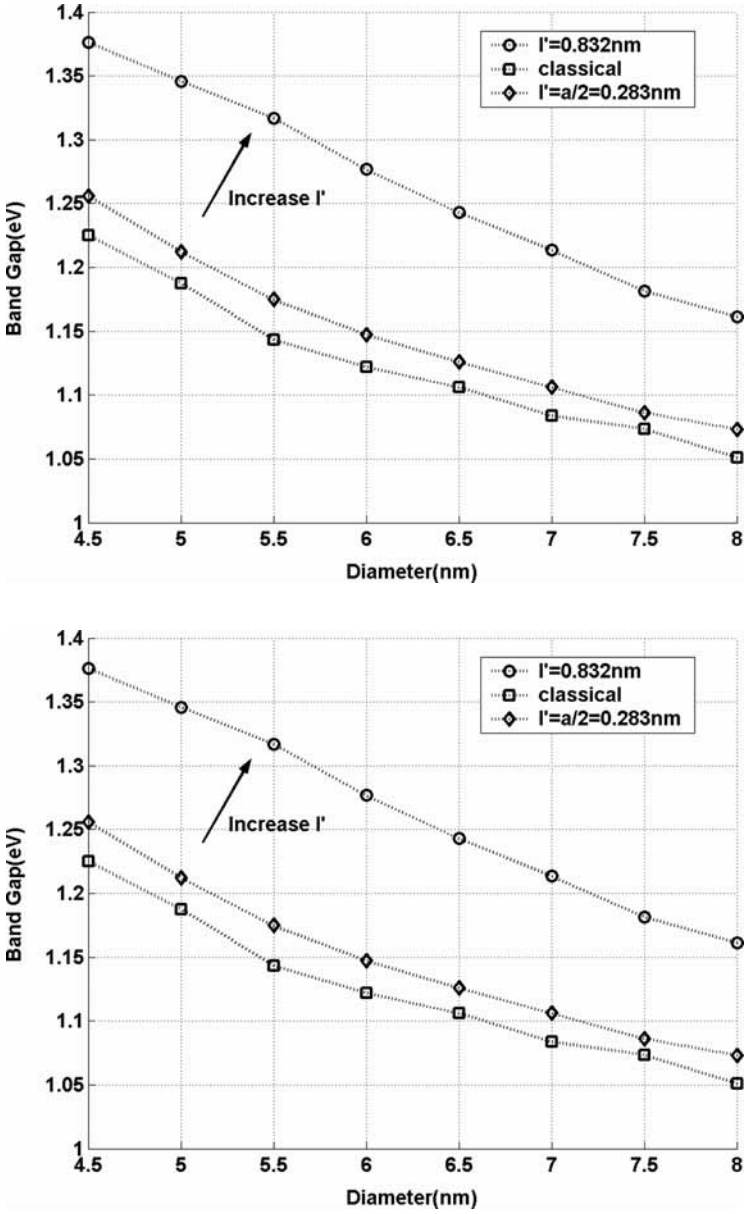

Fig. 4 Band gap of embedded quantum dots with increase of diameter for non-local case with $l' = 0.832\,\text{nm}$ and $a/2 = 0.2826\,\text{nm}$ and classical case

A finite difference method is employed to solve the coupled eight-band eigenvalue equations indicated in the previous equations. The embedded quantum dot system is simulated by using a sphere contained in a cubic box meshed with a grid of $50 \times 50 \times 50$. The size of the box is chosen to be large enough to justify an 'infinite matrix' approximation, as used to derive the strain field in the previous section. The box size (in which the quantum dot is embedded) is chosen to be $36\,\text{nm} \times 36\,\text{nm} \times 36\,\text{nm}$. Dirichlet boundary conditions are applied at the outer boundary of the box. The discrete model contains 125 000 nodes. Based on the obtained large-scale eigenvalue linear system, the Jacobi–Davidson (JD) method [**84**] is used to extract the eigen-energies. Since only the eigenvalues near the smallest conduction band and largest valence band are sought, a shift-invert method is used, which searches the eigenvalues around the desired target energy.

4 RESULTS AND DISCUSSION

In Fig. 3, the zero k (band edge) profile is plotted and results are compared for both classical elasticity-based results and non-local elasticity. It can be observed that the non-local elasticity gives a non-uniform band edge profile inside the quantum dot in contrast to the classical result, which is similar to that obtained in references [**38**] and [**85**].

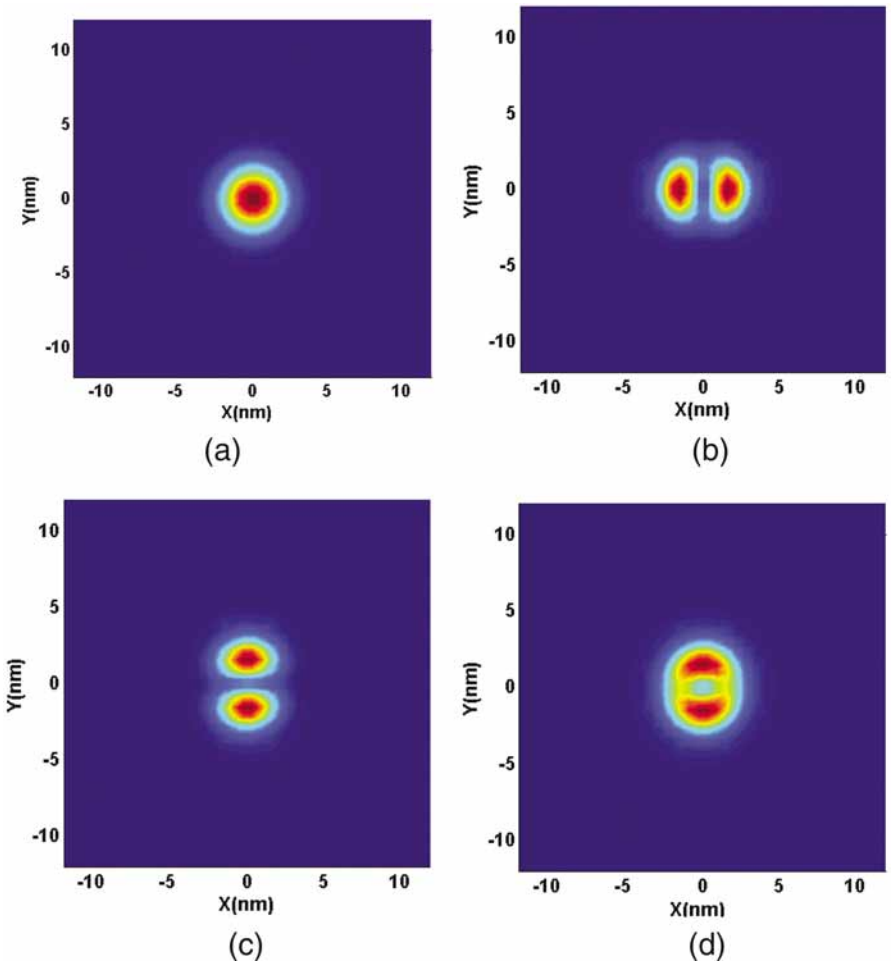

Fig. 5 Magnitude of wave function $\sum_{i=1..8} |\psi_i(r)|$ for quantum dot ($R_0 = 3.5$ nm), first four lowest conduction bands: (a) ground state, (b), (c), and (d) are the 1st, 2nd, and 3rd excited states

Band edge profile is very useful to determine the confinement condition of carriers. In Fig. 3, electrons and holes are all confined in each of the bands, both in classical and non-local elasticity cases. This is despite the fact that there are large differences between these two theories, especially around the interface.

Figure 4 depicts the energy band gap (the lowest conduction energy minus the highest valence energy) versus size. Clearly, the non-local strain effects induce an additional size dependency in the quantum confinement size effect.

Interestingly, the deviation of band gap in the non-local case from the classical result can be as high as 150 meV for a quantum dot with radius of 3 nm. A difference of 100 meV still exists between the non-local and classical results for a quantum dot with radius up to 4 nm. As mentioned above, there is uncertainity in the estimation of the length scale. A conservative estimate of $l' = a/2 = 0.2826$ nm is also chosen. A band gap difference from the classical solution of 30 meV still exists for a quantum dot with diameter of 6 nm. Considering the intervalence bands transition energy is only around 10 meV, 30 meV is indeed a large difference.

A band gap of 1.33 eV has been reported previously [**86**] for a quantum dot with diameter around 4.22 nm. The present calculation gives a value of 1.37 eV for $l' = 0.832$, 1.27 eV for $l' = 0.2826$, and 1.24 eV for the classical case. It can only be said that all the calculations approach the true result. However, the strain calculation in reference [**86**] is based on the Keating valence force field. It is a two-parameter force field and is not accurate for incorporating dispersive (non-local) effects, as indicated by Keating himself [**61**]. There are other force fields which perhaps are better for inclusion of the dispersive (non-local) effect, such as Herman's force field [**87**]. Hence, calculation based on reference [**87**], other more appropriate empirical forced fields, or, more ideally, *ab initio* methods could be employed. This is currently under investigation by the authors.

Apart from the energy spectra, the confinement condition for electrons and holes is presented below. In Fig. 5, the magnitude of wave function for

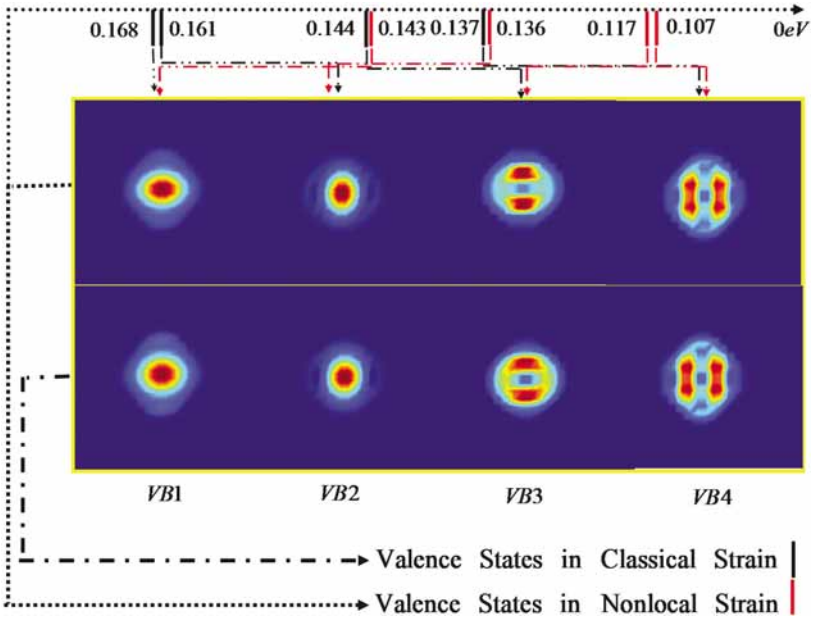

Fig. 6 Magnitude of wave function $\sum_{i=1..8} |\psi_i(r)|$ for quantum dot ($R_0 = 3.5$ nm), first four highest valence bands

electrons in conduction bands is shown for a quantum dot with radius equal to 3.5 nm (with strain taken from non-local elasticity). The contour plots are in the x–y plane and since there is barely any qualitative difference between the non-local and classical elasticity cases, only the former is shown here.

As can be seen from Fig. 5, the carriers are confined in the quantum dot for all the bands shown above. The ground state conduction band shows wave function with s-like symmetry, as expected from the empirical pseudopotential method [**86**]. The splitting of the wave function can be observed in higher excited states. Similarly, wave functions for valence states are presented in Fig. 6.

5 CONCLUSIONS

In conclusion, in the present work, a detailed electronic band structure calculation has been provided for the InAs–GaAs quantum dot system that duly incorporates size effects in the mechanical strain at the nanoscale owing to dispersive (non-local) effects. There is some uncertainty as to the true magnitude of non-local effects; despite that, even for conservative estimates, large quantitative differences in the calculated band gaps are found when the aforementioned size effects are included. No significant qualitative differences are found, although some tentative evidence exists (to be explored in future works) that incorporation of the non-local strain effects may help to eliminate spurious solutions that often arise in the use of the multiband envelope function approach.

REFERENCES

1 **Nakamura, S., Pearton, S.,** and **Fasol, G.** In *The blue laser diode: the complete story*, 2002 (Springer, Berlin).
2 **Arakawa, Y.** Progress in GaN-based quantum dots for optoelectronics applications. *IEEE J. Select. Top. Quantum Electron.*, 2002, **8,** 823.
3 **Deppe, D. G.,** and **Huffaker, D. L.** Quantum dimensionality, entropy, and the modulation response of quantum dot lasers. *Appl. Phys. Lett.*, 2000, **77,** 3325.
4 **Bhattacharya, P.** Quantum well and quantum dot lasers: from strained-layer and self-organized epitaxy to high-performance devices. *Opt. Quant. Election.*, 2000, **32,** 211.
5 **Chye, Y., White, M. E., Johnston-Halperin, E., Gerardot, B. D., Awschalom, D. D.,** and **Petroff, P. M.** Spin injection from (Ga, Mn) As into InAs quantum dots. *Phys. Rev. B*, 2002, **66,** 201–301.
6 **Lundstrom, T., Schoenfeld, W., Lee, H.,** and **Petroff, P. M.** Exciton storage in semiconductor self-assembled quantum dots. *Science*, 1999, **286,** 2312.
7 **Petroff, P. M.** Single quantum dots. Fundamentals, applications, and new concepts. *Top. Appl. Phys.*, 2003, **90,** 1.
8 **Alivisatos, P.** *Semiconductor nanocrystals: from scaling laws to biological applications*, 2000.
9 **Bhattacharya, P., Stiff-Roberts, A. D., Krishna, S.,** and **Kennerly, S.** Quantum dot infrared detectors and sources. *Int. J. High Speed Electron. Systems*, 2002, **12,** 969.
10 **Bimberg, D., Grundmann, M.,** and **Ledentsov, N. N.** *Quantum dot heterostructures*, 1996 (Wiley, New York).
11 **Davies, J. H.** *The physics of low-dimensional semiconductors: an introduction*, 2000 (Cambridge University Press, Cambridge).

12 **Singh, J.** *Physics of semiconductors and their heterostructures*, 1992 (McGraw-Hill Higher Education).
13 **Yu, P. Y.** and **Cardona, M.** *Fundamentals of semiconductors: physics and materials properties (Advanced Text in Physics)*, 3rd Edition, 2004 (Springer).
14 **Bastard, G.** *Wave mechanics applied to semiconductor heterostructures*, 1st Edition, 1991 (Wiley, Chichester).
15 **Kane, E. O.** In *Semiconductors and semimetals, physics of III–V compounds* (Eds R. K. Williardson and A. C. Beer), Vol. 1, 1966 (Academic Press, New York).
16 **Sercel, P. C.** and **Vahala, K. J.** Analytical formalism for determining quantum-wire and quantum-dot band structure in the multiband envelope-function approximation. *Phys. Rev. B*, 1990, **42,** 3690.
17 **Efros, A. L.** and **Rosen, M.** Quantum Size Level Structure of Narrow-gap Semiconductor Nanocrystals: Effect of Band Coupling. *Phys. Rev. B.*, 1998, **58,** 7120.
18 **Gashimzade, F. M., Babaev, A. M.,** and **Bagirov, M. A.** Energy spectra of narrow- and zero- gap semiconductor quantum dots. *J. Phys.: Condens. Matt.* **12,** 7923.
19 **Sercel, P. C., Efros, A. L.,** and **Rosen, M.** Intrinsic gap states in semiconductro nanocrystals. *Phys. Rev. Lett.*, 1999, **83,** 2394.
20 **Pryor, C.** Eight-band calculations of strained InAs/GaAs quantum dots compared with one-, four-, and six-band approximations. *Phys. Rev. B*, 1998, **57,** 7190.
21 **Stier, O., Grundmann, M.** and **Bimberg, D.** Electronic and optical properties of strained quantum dots modeled by 8-band k.p theory. *Phys. Rev. B*, 1999, **59,** 5688.
22 **Burt, M. G.** The justification for applying the effective-mass approximation to microstructures. *J. Phys.: Cond. Matter*, 1992, **4,** 6651.
23 **Burt, M. G.** Fundamentals of envelope function theory for electronic states and photonic modes in nanostructures. *J. Phys.: Condens. Matt.*, 1999, **11,** R53.
24 **Bastard, G.** Superlattice band structure in the envelope-function approximation. *Phys. Rev. B*, 1981, **24,** 5693.
25 **Lin-Liu, Y. R.** and **Sham, L. J.** Interface states and subbands in HgTe–CdTe heterostructures. *Phys. Rev. B*, 1985, **32,** 5561.
26 **Baraff, G. A.** and **Gershoni, D.** Eigenfunction-expansion method for solving the quantum-wire problem: formulation. *Phys. Rev. B*, 1991, **43,** 4011.
27 **Chao, C. Y.-P.,** and **Chuang, S. L.** Spin-orbit-coupling effects on the valence-band structure of strained semiconductor quantum wells. *Phys. Rev. B*, 1992, **46,** 4110.
28 **Edwards, G., Valadares, E. C.,** and **Sheard, F. W.** Hole subband states of GaAs/AlxGa1–xAs quantum wells within the 6×6 Luttinger model. *Phys. Rev. B*, 1994, **50,** 8493.
29 **Foreman, B. A.** Effective-mass Hamiltonian and boundary conditions for the valence bands of semiconductor microstructures. *Phys. Rev. B*, 1993, **48,** 4964.
30 **Foreman, B. A.** Elimination of spurious solutions from eight-band k.p theory. *Phys. Rev. B*, 1997, **56,** R12748.
31 **van Dalen, R.** and **Stavrinou, P. N.** General rules for constructing valence band effective mass Hamiltonians with correct operator ordering for heterostructures with arbitrary orientations. *Semiconductor. Sci. Technol.*, 1998, **13,** 11.
32 **Mireles, F.** and **Ulloa, S. E.** Ordered Hamiltonian and matching conditions for heterojunctions with wurtzite symmetry: GaN/AlxGa1–xN quantum wells. *Phys. Rev. B*, 1999, **60,** 13659.
33 **Mireles, F.** and **Ulloa, S. E.** Strain and crystallographic orientation effects on the valence subbands of wurtzite quantum wells. *Phys. Rev. B*, 2000, **62,** 2562.
34 **Pollak, F. H.** Effects of homogeneous strain on the electronic and vibrational levels in semiconductors. *Semiconduct. Semimet.*, 1990, **32,** 17.
35 **Zhang, Y.** Motion of electrons in semiconductors under inhomogeneous strain with application to laterally confined quantum wells. *Phys. Rev. B*, 1994, **49,** 14352.
36 **Johnson, H. T., Freund, L. B., Akyuz, C. D.,** and **Zaslavsky, A.** Finite element analysis of strain effects on electronic and transport properties in quantum dots and wires. *J. Appl. Phys.* 1998, **84,** 3714.
37 **Grundmann, M., Stier, O.,** and **Bimberg, D.** InAs/GaAs pyramidal quantum dots: strain distribution, optical phonons, and electronic structure. *Phys. Rev. B*, 1995, **52,** 11969.
38 **Yang, M., Strum, J. C.** and **Provost, J.** Calculation of band alignments and quantum confinement effects in zero- and one-dimensional pseudomorphic structures. *Phys. Rev. B*, 1997, **56,** 1973.
39 **Downes, J. R., Faux, D. A.,** and **O'Reilly, E. P.** A simple method for calculating strain distributions in quantum dot structures. *J. Appl. Phys.*, 1997, **1,** 6700.
40 **Andreev, A. D., Downes, J. R., Faux, D. A.,** and **O'Reilly, E. P.** Strain distributions in quantum dots of arbitrary shape. *J. Appl. Phys.*, 1999, **86,** 297.
41 **Pearson, G. S.** and **Faux, D. A.** Analytical solutions for strain in pyramidal quantum dots. *J. Appl. Phys.*, 2000, **88,** 730.
42 **Glas, F.** Elastic relaxation of truncated pyramidal quantum dots and quantum wires in a half space: an analytical calculation. *J. Appl. Phys.*, 2001, **90,** 3232.
43 **Romanov, A. E., Beltz, G. E., Fischer, W. T., Petroff, P. M.,** and **Speck, J. S.** Elastic fields of quantum dots in subsurface layers. *J. Appl. Phys.*, 2001, **89,** 4523.
44 **Pan, E.** and **Yang, B.** Elastostatic fields in an anisotropic substrate due to a buried quantum dot. *J. Appl. Phys.*, 2001, **90,** 6190.
45 **Ellaway, S. W.** and **Faux, D. A.** Effective elastic stiffnesses of InAs under uniform strain. *J. Appl. Phys.*, 2002, **92,** 3027.
46 **Davies, J. H.** Elastic and piezoelectric fields around a buried quantum dot: a simple picture. *J. Appl. Phys.*, 1998, **84,** 1358.
47 **Davies, J. H., Bruls, D. M., Vugs, J. W. A. M.,** and **Koenraad, P. M.** Relaxation of a strained quantum well at a cleaved surface. *J. Appl. Phys.*, 2002, **91,** 4171.
48 **Johnson, H. T.** and **Freund, L. B.** The influence of strain on confined electronic states in semiconductor quantum structures. *Int. J. Solids. Structs*, 2001, **38,** 1045.
49 **Johnson, H. T., Nguyen, V.,** and **Bower, A. F.** Simulated self-assembly and optoelectronic properties of InAs/GaAs quantum dot arrays. *J. Appl. Phys.*, 2002, **92,** 4653.

50 Nishi, K., Yamaguchi, A. A., Ahopelto, J., Usui, A., and **Sakaki, H.** Analyses of localized confinement potential in semiconductor strained wires and dots buried in lattice-mismatched materials. *J. Appl. Phys.*, 1994, **76,** 7437.

51 Pryor, C., Pistol, M. E., and **Samuelson, L.** Electronic structure of strained InP/$Ga_{0.51}In_{0.49}P$ quantum dots. *Phys. Rev. B*, 1997, **56,** 10404.

52 Pryor, C. Eight-band calculations of strained InAs/GaAs quantum dots compared with one-, four-, and six-band approximations. *Phys. Rev. B*, 1998, **57,** 7190.

53 Pryor, C., Kim, J., Wang, L. W., Williamson, A. J., and **Zunger, A.** Comparison of two methods for describing the strain profiles in quantum dots. *J. Appl. Phys.*, 1998, **83,** 2548.

54 Tadi'c, M., Peeters, F. M., Janssens, K. L., Korkusi'nski, M., and **Hawrylak, P.** Strain and band edges in single and coupled cylindrical InAs/GaAs and InP/InGaP self-assembled quantum dots. *J. Appl. Phys.*, 2002, **92,** 5819.

55 Korkusi'nski, M. and **Hawrylak, P.** Electronic structure of vertically stacked self-assembled quantum disks. *Phys. Rev. B*, 2001, **63,** 195311.

56 Shin, H., Lee, W., and **Yoo, Y. H.** Comparison of strain sields in truncated and un-truncated quantum dots in stacked InAs/GaAs nanostructures with varying stacking periods. *J. Phys. Condens. Matt.*, 2003, **15,** 3689.

57 Bellaiche, S. H., Wei, L., and **Zunger, A.** Localization and percolation in semiconductor alloys: GaAsN vs GaAsP. *Phys. Rev. B*, 1996, **54,** 17568.

58 Bernard, J. and **Zunger, A.** Is there an elastic anomaly for a (001) monolayer of InAs embedded in GaAs? *Appl. Phys. Lett.*, 1994, **65,** 165.

59 Cusack, M., Briddon, P., and **Jaros, M.** Electronic structure of InAs/GaAs self-assembled quantum dots. *Phys. Rev. B*, 1996, **54,** R2300.

60 Jiang, H. and **Singh, J.** Strain distribution and electronic spectra of InAs/GaAs self-assembled dots: an eight-band study. *Phys. Rev. B*, 1997, **56,** 4696.

61 Keating, P. N. Effect of invariance requirements on the elastic strain energy of crystals with application to the diamond structure. *Phys. Rev.*, 1966, **145,** 637.

62 Martin, R. M. Elastic properties of ZnS structure semiconductors. *Phys. Rev. B*, 1970, **1,** 4005.

63 Stillinger, F. H. and **Weber, T. A.** Computer simulation of local order in condensed phases of silicon. *Phys. Rev. B*, 1985, **31,** 5262.

64 Yu, W. and **Madhukar, A.** Molecular dynamics study of coherent island energetics, stresses, and strains in highly strained epitaxy. *Phys. Rev. Lett.*, 1997, **79,** 905.

65 Yu, W. and **Madhukar, A.** Molecular dynamics study of coherent island energetics, stresses, and strains in highly strained epitaxy. *Phys. Rev. Lett.*, 1997, **79,** 4939.

66 Makeev, M. A. and **Madhukar, A.** Stress and strain fields from an array of spherical inclusions in semi-infinite elastic media: Ge nanoinclusions in Si. *Phys. Rev. B*, 2003, **67,** 073201.

67 Migliorato, M. A., Cullis, A. G., Fearn, M., and **Jefferson, J. H.** Atomistic simulation of strain relaxation in $In_xGa_{1-x}As$/GaAs quantum dots with nonuniform composition. *Phys. Rev. B*, 2002, **65,** 115316.

68 DiCarlo, A. Microscopic theory of nanostructured semiconductor devices: beyond the envelope-function approximation. *Semiconductor Sci. Technol.*, 2003, **18,** R1.

69 Zunger, A. Pseudopotential theory of semiconductor quantum dots. *Phys. Status Solidi B*, 2001, **224,** 727.

70 Wang, L. W. and **Zunger, A.** Linear combination of bulk bands method for large-scale electronic structure calculations on strained nanostructures. *Phys. Rev. B*, 1999, **59,** 15806.

71 Wang, L. W. and **Zunger, A.** Pseudopotential-based multiband k.p method for 250000-atom nanostructure systems. *Phys. Rev. B*, 1996, **54,** 11417.

72 Zhang, X. and **Sharma, P.** Size dependency of strain in arbitrary shaped, anisotropic embedded quantum dots due to nonlocal dispersive effects. *Phys. Rev. B*, 2005, **72,** 195345-1–195345-16.

73 Sharma, P. and **Ganti, S.** Size-dependent Eshelby's tensor for embedded nano-inclusions incorporating surface/interface energies. *J. Appl. Mechanics*, 2004, **71,** 663.

74 Eringen, C. *Nonlocal continuum field theories*, (Springer, New York).

75 Sharma, P. and **Ganti, S.** Interfacial elasticity corrections to the elastic state of quantum dots. *Phys. Status Solidi (b)*, 2002, **234,** R10.

76 Alizadeh, A., Sharma, P., Ganti, S., LeBoeuf, S. F., and **Tsakalakos, L.** Templated wide band-gap nanostructures. *J. Appl. Phys.*, 2004, **95,** 8199.

77 Kleinert, H. *Gauge fields in condensed matter*, Vol. 2, 1989 (World Scientific).

78 Bir, G. L. and **Pickus, G. E.** *Symmetry and strain induced effects in semiconductors*, 1974 (John Wiley, New York).

79 Bahder, T. B. Analytic dispersion relations near the Γ point in strained zinc-blended crystals. *Phys. Rev. B*, 1992, **45,** 1629.

80 Zunger, A. Electronic-structure theory of semiconductor quantum dots. *MRS Bull.*, 1998, 35.

81 Bahder, T. B. Eight-band k.p model of strained zinc-blended crystals. *Phys. Rev. B*, 1992, **41,** 11992.

82 Stier, O. *Berlin Studies in Solid State Physics 7: Electronic and Optical Properties of Quantum Dots and Wires*, 2000 (Wissenschaft & Technik).

83 DiVincenzo, D. P. Dispersive corrections to continuum elastic theory in cubic crystals. *Phys. Rev. B*, 1986, **34,** 5450.

84 Sleijpen, G. and **Vorst, H.** A generalized Jacobi–Davidson iteration method for linear eigenvalue problems. *SIAM J. Matt. Analysis Appl.*, 1996, **17,** 2.

85 Holm, M., Pistol, M., and **Pryor, C.** Calculations of the electronic structure of strained InAs quantum dots in InP. *J. Appl. Phys.*, 2002, **92,** 932.

86 Williamson, A. J. and **Zunger, A.** InAs quantum dots: predicted electronic structure of free-standing versus GaAs-embedded structures. *Phys. Rev. B*, 1999, **59,** 15819.

87 Herman, F. Lattice vibrational spectrum of germanium. *J. Phys. Chem. Solids*, 1959, **8,** 405.